Exploring Inner-sphere Water Interactions of Fe(II) and Co(II) Complexes of 12-Membered Macrocycles to Develop CEST MRI Probes

Christopher J. Bond, Gregory E. Sokolow, Matthew R. Crawley, Patrick J. Burns, Jordan M. Cox,‡ Ramasamy Mayilmurugan,† and Janet R. Morrow*

Department of Chemistry, University at Buffalo, State University of New York, Amherst NY 14260, USA

Abstract

Several paramagnetic Co(II) and Fe(II) macrocyclic complexes were prepared with the goal of introducing a bound water ligand to produce paramagnetically shifted water ^{1}H resonances and for paraCEST applications (paraCEST = paramagnetic chemical exchange saturation transfer). Three 12-membered macrocycles with amide pendent groups including 1,7-bis(carbamoylmethyl)-1,4,7,10-tetraazacyclodocane (DCMC), 4,7,10-tris(carbamoylmethyl)-,4,7,10-triaza-12-crown-ether (N3OA), 4,10-bis(carbamoylmethyl)-4,10-diaza-12-crown-ether (NODA) were prepared and their Co(II) complexes were characterized in the solid state and in solution. The crystal structure of $[Co(DCMC)]Br_2$ featured a six-coordinate Co(II) center with distorted octahedral geometry, while $[Co(NODA)(OH_2)]Cl_2$ and $[Co(N3OA)](NO_3)_2$ were seven coordinate. The analogous Fe(II) complexes of NODA and NO3A were successfully prepared, but the complex of DCMC oxidized rapidly to the Fe(III) form. Similarly, $[Fe(NODA)]^{2+}$oxidized over several days, forming crystals of the Fe(III) complex isolated as the μ-O bridged dimer. Magnetic susceptibility values and paramagnetic NMR spectra of the Fe(II) complexes of NODA and N3OA as well as Co(II) complexes of DCMC, NODA, and N3OA were consistent with high spin complexes. CEST peaks ranging from 60 to 70 ppm attributed to NH groups of the amide pendents were identified. Variable temperature ^{17}O NMR spectra of Co(II) and Fe(II) NODA complexes were consistent with rapid exchange of the water ligand with bulk water. Notably, the Co(II) and Fe(II) complexes presented here produced substantial paramagnetic shifts of bulk water ^{1}H resonances, independent of having an inner-sphere water.

‡Current address: Department of Chemistry and Chemical Biology, Northeastern University, Boston, MA, 02115

†Current address: School of Chemistry, Madurai Kamaraj University, Madurai 625021, India

Introduction

Most MRI(magnetic resonance imaging) contrast agents contain paramagnetic metal ion complexes that interact with water through inner-sphere and outer-sphere modes.[1-2] While most studies focus on inner-sphere interactions, it is appreciated that outer-sphere, or more specifically, second-sphere interactions are also important.[3] Several recent reports show the importance of second-sphere interactions in T_1 relaxivity agents that contain Gd(III)[4-5] and also in paraCEST (paramagnetic chemical exchange saturation transfer) complexes that contain Eu(III), Yb(III), Ni(II) or Co(II).[6-9] Another type of contrast agent for which second-sphere complexes are critically important are nano-sized carriers.[10] Such nano-carriers have assemblies of protons that interact with the paramagnetic complex. Common examples include liposomes loaded with lanthanide complexes[11], silica particles with attached lanthanide complexes[12] or cells containing lanthanide shift agents.[13] The paramagnetic metal complex in the nano-carrier produces a shifted pool of protons. Magnetically saturating the shifted pool of water protons with a presaturation pulse, followed by exchange of saturated protons with bulk water protons decreases the intensity of the water signal. These nano-sized CEST contrast agents are promising for applications requiring increased sensitivity.[14]

Current research in our laboratory focuses on development of transition metal ion complexes as MRI contrast agents.[15-21] We recently reported transition metal complexes with inner-sphere water ligands that were developed with the goal of shifting the water proton resonances in the interior of liposomes or cells.[7-8] Towards this goal, we showed that certain Co(II) complexes produce substantial proton water shifts.[8] Paramagnetic Ni(II) complexes are also effective water proton shift agents, although the smaller magnetic susceptibility of these complexes produces less-shifted protons.[7] One of the most intriguing results from these studies was that outer-sphere water interactions contributed substantially to bulk water proton paramagnetic shifts, especially for complexes with alcohol donor groups. As a result of these studies, we began to question whether inner-sphere waters were necessary to obtain substantial paramagnetic induced proton water shifts from transition metal ion complexes.

Towards the further development of transition metal complexes as shift reagents for water ^{1}H resonances, ligands related to the 12-membered tetraaza-macrocycle with four amide pendents (TCMC in Scheme 1) were studied. The TCMC ligand forms an interesting series of complexes with transition metal ions ranging from eight-coordinate Fe(II)[18] or Mn(II)[22] to seven or six-coordinate Co(II) to six-coordinate Ni(II).[18] The Fe(II) complexes of TCMC are especially inert to metal ion release as well as highly stabilized in the divalent form, preventing oxidation to Fe(III).[15, 23] Neither the Fe(II), Co(II) or Ni(II) complexes have bound water in the solid state, as shown by x-ray crystallography.[18] In the work

presented here, the number of donor groups in the ligand is reduced from eight to six or seven donor groups with the aim of producing an inner-sphere water. Our complexes contain Fe(II) or Co(II) with either tetra-aza or mixed aza-oxa 12-membered macrocyclic complexes with pendent amides (Scheme 1).

The isolation and solution characterization of Co(II) or Ni(II) complexes with bound water ligands is relatively straightforward, but what of Fe(II) complexes? Fe(II) complexes are of special interest given the important place of iron in biological systems and their potential in the development of new contrast agents. Notably, it is challenging to develop ligands that form stable, high spin Fe(II) complexes in aqueous solution. Neutral donor groups such as amides, alcohols and picolyl groups successfully stabilize the divalent state.[15, 24-28] Complexes studied in our labs to date have featured an encapsulated Fe(II) center to better control oxidation and spin state, and we have avoided inner-sphere water ligands.[17-20, 24, 26, 29-31] However, there are a few literature examples of Fe(II) complexes that are stable in aqueous solution and have a bound water ligand. For example, the solution chemistry of polyaminocarboxylate complexes of Fe(II) with a bound water have been studied by Rudi van Eldik.[32-33] These complexes have a rapidly exchanging water ligand, but are air sensitive. An Fe(II) complex with pyrazole donors was shown to have a water ligand that gives rise to a CEST effect, signifying a slowly exchanging water ligand.[34] In this study, we present a comparison of Fe(II) and Co(II) complexes of 12ane macrocycles and highlight the challenges of developing Fe(II) complexes as water proton shift agents.

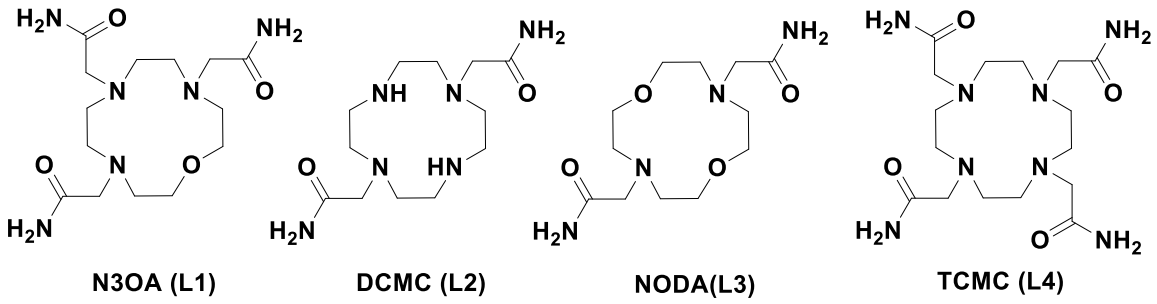

Scheme 1

RESULTS

Synthesis and structure of complexes. Three new macrocyclic ligands with pendent amide groups were synthesized (NO3A, DCMC, NODA) for comparison with the reported tetraaza-macrocycle,

TCMC (Scheme 1). Synthetic schemes are shown in the supplementary section (Scheme S1). The mixed aza-oxa ligands, N3OA and NODA were prepared by alkylation of the unsubstituted macrocycles with bromoacetamide. The macrocycle DCMC was prepared from alkylation of a 1,7-protected cyclen (1,4,7,10-tetraazacyclododecane) precursor followed by deprotection using catalytic hydrogenation. The Co(II) complexes were synthesized by addition of $Co(NO_3)_2$ or $CoCl_2$ to the neutral macrocycles N3OA, DCMC, or NODA in acetonitrile or ethanol (Scheme S2). All Co(II) complexes were crystallized and their structures are presented here.

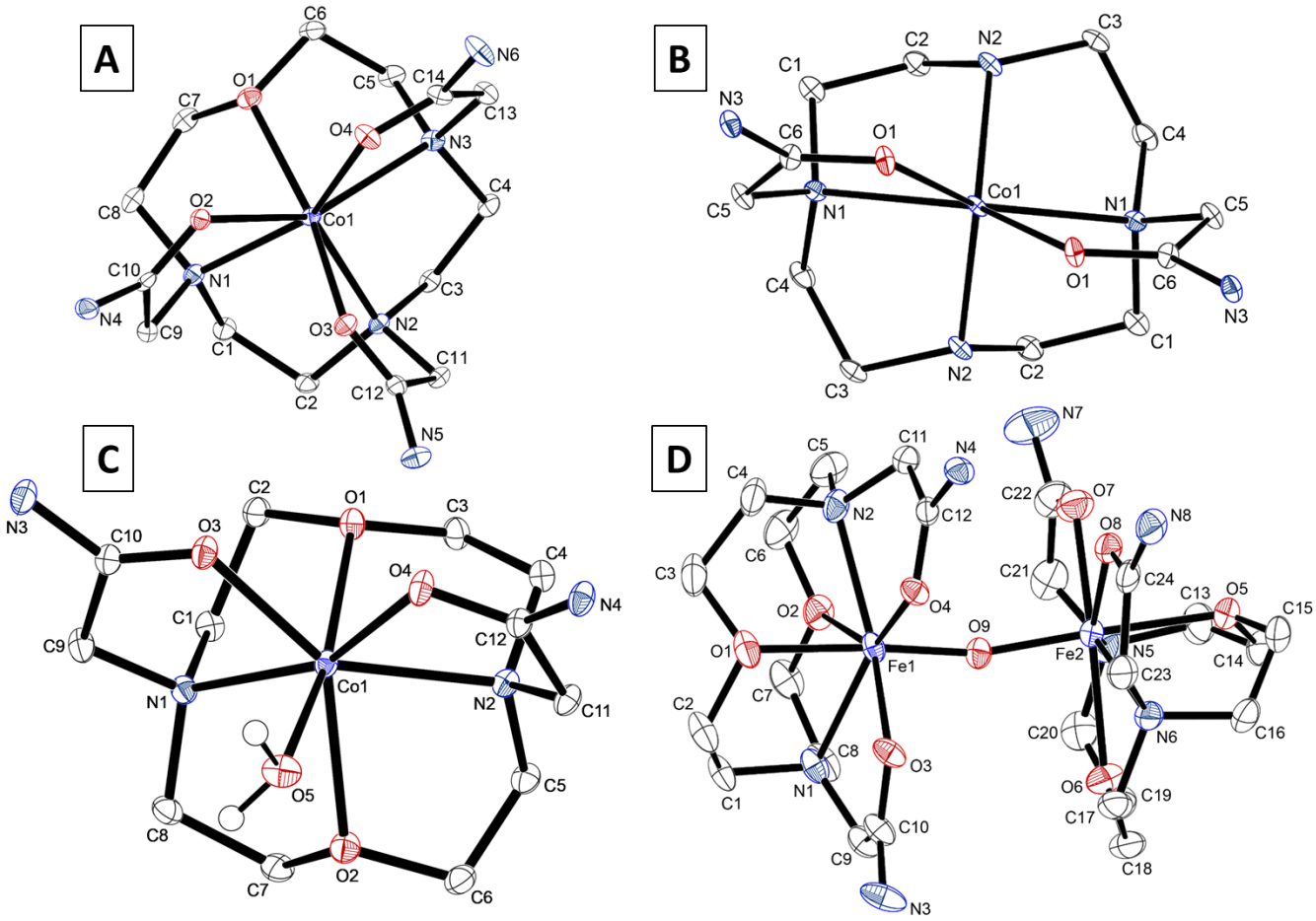

Figure 1. ORTEP plots of the crystal structure of $[Co(N3OA)] \cdot 2.33H_2O$ (A), $Co(DCMC)Br_2$ (B), $[Co(NODA)(H_2O)]Cl_2$ (C), and $[Fe_2(NODA)_2(O)](CF_3SO_3)_4$ dimer (D) (at the 50 % probability level). Hydrogen atoms, counterions, and water molecules of crystallization have been omitted for clarity.

The cationic $[Co(N3OA)]^{2+}$ complex has all four macrocycle donors bound to the Co(II) and all three pendent amides bound through carbonyl oxygen atoms. Both enantiomers are found in the crystal structure, as evident by the centrosymmetric space group *P*–1. The complexes presented here possess highly distorted coordination environments making it difficult to classify them within the "typical"

coordination polyhedral. $[Co(N3OA)]^{2+}$ can best be described as having a capped trigonal prismatic geometry, analogous to, though distorted from, the geometry of TaF_7.[2–35] Two formula units comprise the asymmetric unit, one of which exhibited pseudorotational disorder of the macrocyclic ligand over two positions differing by 20(3)° in a ratio of 68:32. A complex hydrogen bond network connects each formula to the nitrate counterions, along with co-crystallized water units. The structure of $[Co(DCMC)]^{2+}$ has four Co(II)-nitrogen bonds to the macrocycle backbone and two amide carbonyl groups. The six-coordinate complex has an average twist angle of 11.7° between the two trigonal planes, consistent with a distorted trigonal prismatic structure (Figures 1B and S1). The Co(II) center of the cationic $[Co(NODA)(OH_2)]^{2+}$ complex is bound to all donor atoms of the macrocycle, the two pendent amide groups, and a water ligand. The geometry of the complex resembles a distorted pentagonal pyramidal structure, with the coordinated water molecule (O-5) and (O-1) of the ring forming the axial atoms, with a bond angle of 168.23°. The solid state structure reveals an intricate hydrogen bond network from the coordinated H_2O moiety to both the Cl^- counterion, as well as additional uncoordinated water units. Furthermore, intermolecular hydrogen bonding was observed between formula units between adjacent amide arms. Selected bond lengths and angles are in Table 1, and crystallographic data is given in Table S1.

Table 1. Selected metal bond lengths (top) and bond angles of the $[Co(N3OA)](NO_3)_2 \cdot 2.33H_2O$ $[Co(DCMC)]Br_2$, $[Co(NODA)(OH_2)]Cl_2 \cdot 2H_2O$, and $[Fe_2(NODA)_2(O)](CF_3SO_3)_3$ crystals.

Selected Bond Lengths

$[CoN3OA)](NO_3)_2 \cdot 2.33H_2O$			$[Co(DCMC)]Br_2$			$[Co(NODA)(OH_2)]Cl_2 \cdot 2H_2O$			$[Fe_2(NODA)_2(O)](CF_3SO_3)_4$		
Atom1	Atom 2	Distance (Å)	Atom1	Atom 2	Distance (Å)	Atom1	Atom 2	Distance (Å)	Atom1	Atom 2	Distance (Å)
Co1A	O2A	2.143(2)	Co1	O1	2.079	Co1	O1	2.364(1)	Fe1	O1	2.124(1)
Co1A	O3A	2.141(1)	Co1	N1	2.322	Co1	O2	2.237(1)	Fe1	O2	2.347(1)
Co1A	O1A	2.320(2)	Co1	N2	2.113	Co1	O3	2.149(1)	Fe1	O3	2.151(1)
Co1A	O4A	2.14(1)	Co1	O1	2.079	Co1	O4	2.110(1)	Fe1	O4	2.129(1)
Co1A	N1A	2.211(3)	Co1	N1	2.322	Co1	O5	2.115(1)	Fe1	O9	1.7776(9)
Co1A	N2A	2.292(3)	Co1	N2	2.113	Co1	N1	2.229(1)	Fe1	N1	2.276(1)
Co1A	N3A	2.234(2)				Co1	N2	2.236(1)	Fe1	N2	2.266(2)

Selected Bond Angles

$[CoN3OA)](NO_3)_2 \cdot 2.33H_2O$				$[Co(DCMC)]Br_2$				$[Co(NODA)(OH_2)]Cl_2 \cdot 2H_2O$				$[Fe_2(NODA)_2(O)](CF_3SO_3)_4$			
Atom1	Atom 2	Atom 3	Angle (°)	Atom1	Atom 2	Atom 3	Angle (°)	Atom1	Atom 2	Atom 3	Angle (°)	Atom1	Atom 2	Atom 3	Angle (°)
O2A	Co1A	O3A	78.16	O1	Co1	N1	75.3	O1	Co1	O2	116.68	O1	Fe1	O2	91.26
O2A	Co1A	O1A	77.55	O1	Co1	N2	98.6	O1	Co1	O3	127.09	O1	Fe1	O3	81.11
O2A	Co1A	O4A	78.4	O1	Co1	O1	83.2	O1	Co1	O4	141.20	O1	Fe1	O4	86.89
O2A	Co1A	N1A	78.6	O1	Co1	N1	151.3	O1	Co1	O5	74.15	O1	Fe1	O9	176.30
O2A	Co1A	N2A	147.02	O1	Co1	N2	123	O1	Co1	N1	73.75	O1	Fe1	N1	78.00
O2A	Co1A	N3A	135.60	N1	Co1	N2	79.4	O1	Co1	N2	73.57	O1	Fe1	N2	77.89
O3A	Co1A	O1A	152.86	N1	Co1	O1	151.3	O2	Co1	O3	95.22	O2	Fe1	O3	142.77
O3A	Co1A	O4A	85.8	N1	Co1	N1	130.8	O2	Co1	O4	82.07	O2	Fe1	O4	142.54
O3A	Co1A	N1A	87.6	N1	Co1	N2	78.3	O2	Co1	O5	168.22	O2	Fe1	O9	88.76
O3A	Co1A	N2A	75.92	N2	Co1	O1	123	O2	Co1	N1	77.14	O2	Fe1	N1	69.38
O3A	Co1A	N3A	132.57	N2	Co1	N1	78.3	O2	Co1	N2	78.32	O2	Fe1	N2	69.82
O1A	Co1A	O4A	101.0	N2	Co1	N2	124.7	O3	Co1	O4	80.37	O3	Fe1	O4	73.78
O1A	Co1A	N1A	75.9	O1	Co1	N1	75.3	O3	Co1	O5	80.46	O3	Fe1	O9	96.66
O1A	Co1A	N2A	121.0	O1	Co1	N2	98.6	O3	Co1	N1	73.94	O3	Fe1	N1	73.39
O1A	Co1A	N3A	74.27	N1	Co1	N2	79.4	O3	Co1	N2	158.19	O3	Fe1	N2	141.53
O4A	Co1A	N1A	157.0					O4	Co1	O5	86.39	O4	Fe1	O9	95.34
O4A	Co1A	N2A	119.2					O4	Co1	N1	145.02	O4	Fe1	N1	145.54
O4A	Co1A	N3A	74.2					O4	Co1	N2	78.12	O4	Fe1	N2	73.23
N1A	Co1A	N2A	80.2					O5	Co1	N1	111.74	O9	Fe1	N1	98.56
N1A	Co1A	N3A	125.2					O5	Co1	N2	101.64	O9	Fe1	N2	105.57
N2A	Co1A	N3A	77.4					N1	Co1	N2	123.66	N1	Fe1	N2	131.54

The Fe(II) complexes of N3OA were prepared with $FeCl_2$ in ethanol, whereas complexes of NODA were prepared by addition of $Fe(OTf)_2$ to the macrocycle in acetonitrile. We were not able to obtain crystals of these two complexes. Characterization in aqueous solution by ^1H NMR spectroscopy, mass spectrometry, and magnetic susceptibility are all consistent with high spin Fe(II) as described below. In contrast, the Fe(II) complex of DCMC was readily oxidized in water to produce the Fe(III) complex as described further below. An acetonitrile solution of $[Fe(NODA)]^{2+}$ produced crystals of an Fe(III) complex (Figure 1D) upon standing for several days. The solid state structure features two seven-coordinate Fe(III) centers bridged by a μ-oxide ligand, with a notably shorter bond length than other

coordinating atoms (1.78 vs >2.1Å). The Fe-centers both display distorted pentagonal bipyramidal geometry with an average axial bond angle of 176.40°.

The Co(II) and Fe(II) complexes were characterized in solution by their magnetic susceptibility measurements and ^{1}H NMR spectra. Magnetic moments, as determined by using Evans method, are tabulated in Table 2. The magnetic moments, ranging from 4.1 to 4.4, for the cobalt complexes are consistent with high spin Co(II).[16, 18, 36] Magnetic susceptibility data are consistent with high spin Fe(II) for $[Fe(NODA)]^{2+}$ and $[Fe(N3OA)]^{2+}$ complexes with magnetic moments of 4.5 and 4.7, respectively.[29-30, 36] Additionally, these five complexes all produced the relatively sharp and highly paramagnetically shifted proton resonances that are characteristic of Co(II) and Fe(II) complexes in these types of macrocyclic ligands.[16, 18, 29]

The ^{1}H NMR spectra of the Co(II) and Fe(II) complexes of NODA had relatively sharp, paramagnetically shifted proton resonances at 25 °C (Figure 2 and Figures S2). The five prominent resonances in the NMR spectra in D_2O solutions correspond to four magnetically inequivalent protons on the macrocyclic ring of the complexes and one resonance from the proton of the amide pendent methylene groups, as illustrated by the $[Co(NODA)]^{2+}$ ^{1}H NMR spectrum in Figure 2. The fact that there are only five proton resonances suggests that the complex is dynamic on the NMR timescale. This may involve pendent group movement to interchange the H3 and H3' protons. In H_2O, the exchangeable amide NH proton peaks are observed (Figure 2). However, the ^{1}H resonance of bound water is not observed in this spectrum. The lack of an observed ^{1}H resonance is consistent with rapid water exchange on the NMR timescale as supported below by variable temperature ^{17}O NMR experiments. For $[Fe(NODA)]^{2+}$, the

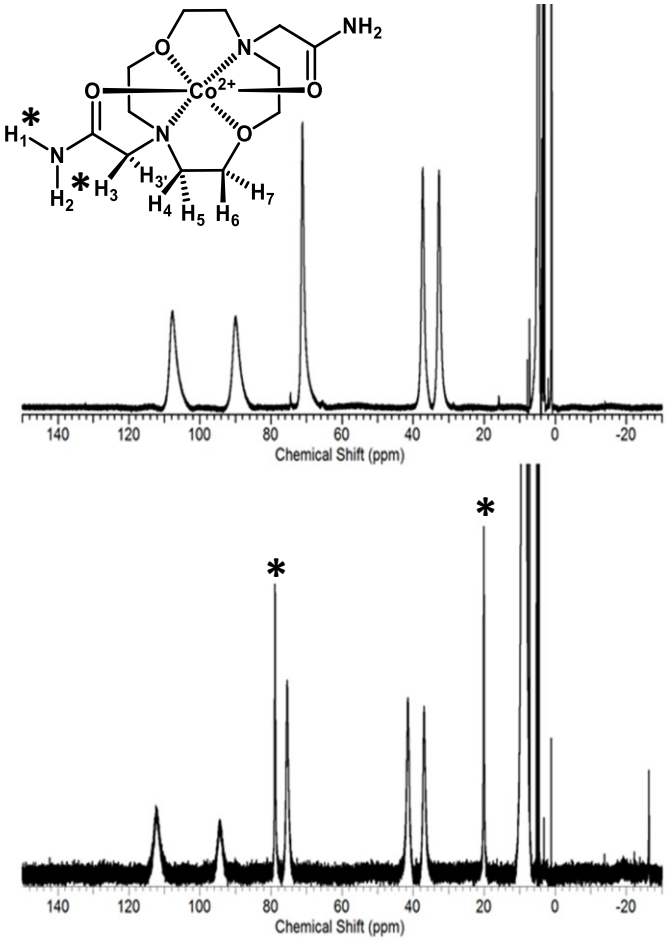

Figure 2. ^{1}H NMR spectra of $[Co(NODA)]^{2+}$ in D_2O (top) and in water (bottom). The bottom spectrum shows exchangeable amide proton resonances, marked with (*).

comparison of spectra in D_2O and aprotic CD_3CN reveals the amide proton peaks (Figure S2).

The very broad proton resonances observed in the ^1H NMR spectra of $[Co(N3OA)]^{2+}$, $[Co(DCMC)]^{2+}$, and $[Fe(N3OA)]^{2+}$are similar to that observed for $[Co(TCMC)]^{2+}$, which has been attributed to a fluxional process.[16, 18] Consistent with a dynamic process, increasing the temperature of the NMR experiments for these complexes produces notably sharper proton resonances. This is shown in Figures S3-S5 for the Co(II) and Fe(II) complexes of N3OA complexes where the resonances at 80 °C for Fe(II) and Co(II) N3OA become progressively well-defined, as temperatures are raised from 25 °C to 80 °C. Similarly, at 25 °C the paramagnetic NMR spectrum of $[Co(DCMC)]^{2+}$ is very broad with just one resonance observed. Increasing the temperature to 80 °C produces 4-5 distinct resonances for $[Co(DCMC)]^{2+}$ in D_2O.

In contrast to the ease of preparation of $[Co(DCMC)]^{2+}$, we failed to isolate an Fe(II) complex of DCMC when the ligand was treated with Fe(II) salts. Dissolution of the complex in D_2O at millimolar concentrations produced ^1H NMR spectra with no discernable proton resonances at 25 °C (Figure S6). T_1 measurements on solutions of the complex at 400 MHz produced a T_1 relaxivity of 1.0 $mM^{-1}s^{-1}$ at 500 MHz (Figure S7), consistent with an Fe(III) complex.[37]

The UV-vis spectra of the Co(II) complexes of N3OA-TCMC are shown in Figures S8-S9. $[Co(NODA)]^{2+}$ and $[Co(N3OA)]^{2+}$ both produce two major barely resolved peaks at about 510 and 480 nm with extinction coefficients of 10 $M^{-1}cm^{-1}$, consistent with d-d transitions of complexes that are Laporte forbidden. The spectrum of $[Co(TCMC)]^{2+}$ has three bands with extinction coefficients of about 10 $M^{-1}cm^{-1}$ in the region of 460-550 nm. Notably, this complex is highly fluxional in solution and was shown to be a mixture of six and seven coordinate complexes in the solid state. $[Co(DCMC)]^{2+}$ has slightly more intense peaks (ε = 65 $M^{-1}cm^{-1}$) at 470-560 nm, which are similar in position and intensity to distorted octahedral Co(II) macrocyclic complexes reported previously.[8, 38]

Electrochemical data shows that the Co(II) complexes do not readily oxidize over the electrochemical range accessible with water as a solvent, with (Figure S10). Typically, Co(II) macrocyclic complexes with amide pendent groups have high Co(II)/Co(III) redox potentials (800-1000 mV vs. NHE) that signify stabilization of the Co(II) state.[15-16] $[Fe(N3OA)]^{2+}$ does not show an oxidation wave under these conditions, consistent with the redox potentials observed for similar complexes such as $[Fe(TCMC)]^{2+}$ that have a redox potential of 800 mV versus NHE in acetonitrile.[15, 23] $[Fe(DCMC)]^{2+/3+}$ produces a cyclic voltammogram with a two sets of waves between 40 mV and 240mV vs. Ag/AgCl (Figure S11), consistent with the presence of two different species in aqueous solution. By contrast, $[Fe(NODA)]^{2+/3+}$ produces a cyclic voltammogram with a quasi-reversible wave with $E_{1/2}$ of 426 mV versus

Ag/AgCl (Figure S12). A solution of $K_4[(Fe(CN)_6]^{4-}$ was run under similar conditions as a standard (Figure S13) and the $E_{1/2}$ (162 mV) was compared to literature values given versus the standard hydrogen electrode (SHE) of 358 mV.[39] From this data, we calculate a redox potential of 588 mV for $[Fe(NODA)]^{2+/3+}$ and two waves in the range of 240 to 400 mV for $[Fe(DCMC)]^{2+/3}$ versus SHE.

Variable temperature ^{17}O NMR studies. All Co(II) complexes and the Fe(II) complexes of N3OA and NODA were studied by ^{17}O NMR spectroscopy to characterize water interactions. Variable temperature experiments are used to study water ligand exchange for determination of exchange rate constants. In this experiment, the ^{17}O NMR resonance shifts and broadens/sharpens as a function of temperature of an aqueous solution spiked with ^{17}O water and containing 10 mM paramagnetic complex. A typical closed coordination sphere complex will produce a ^{17}O resonance that shifts upfield with an increase in temperature due to the temperature dependence of paramagnetic center. A complex with a bound water molecule that is averaging with bulk water typically displays a broader ^{17}O

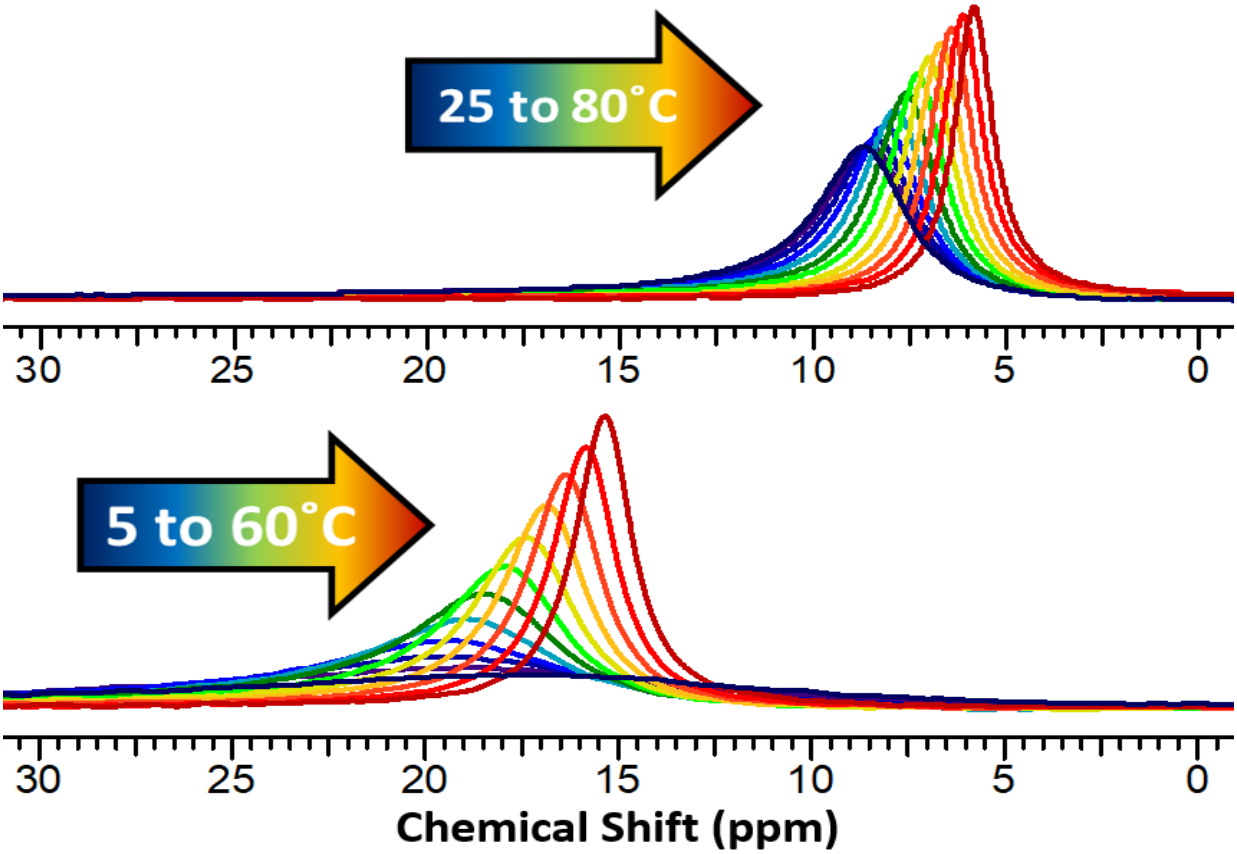

Figure 3. Variable Temperature ^{17}O NMR of 100 mM $[Fe(N3OA)]^{2+}$ (top) from 25 °C to 80 °C and 50 mM $[Fe(NODA)]^{2+}$ from 5 °C to 60 °C (bottom) in 5 degree increments, solutions adjusted to approximately pH 6 and contained 100 mM NaCl.

resonance due to direct interaction of water with the paramagnetic center. An increase in temperature leads to more rapid water exchange, and this will affect the ^{17}O NMR shift and peak width.

The variable temperature spectra of $[Fe(N3OA)]^{2+}$ (top) and $[Fe(NODA)]^{2+}$ (bottom) illustrated in figure 3 demonstrates these striking differences in behavior between complexes with a bound water and those without.[8] The $[Fe(N3OA)]^{2+}$ NMR spectra (Figure 3 top) show little broadening of the water resonance as compared to a water standard (Figure S14), indicating that there is no direct metal-water interaction, and only outer-sphere waters. The $[Fe(NODA)]^{2+}$ spectra show significant peak shifting and broadening, indicative of an inner-sphere metal-water interaction.[32-33] The variable temperature ^{17}O NMR spectra of $[Co(N3OA)]^{2+}$, $[Co(DCMC)]^{2+}$, and $[Co(NODA)]^{2+}$ and corresponding standards are shown in the supplemental section (Figures S14-S18).

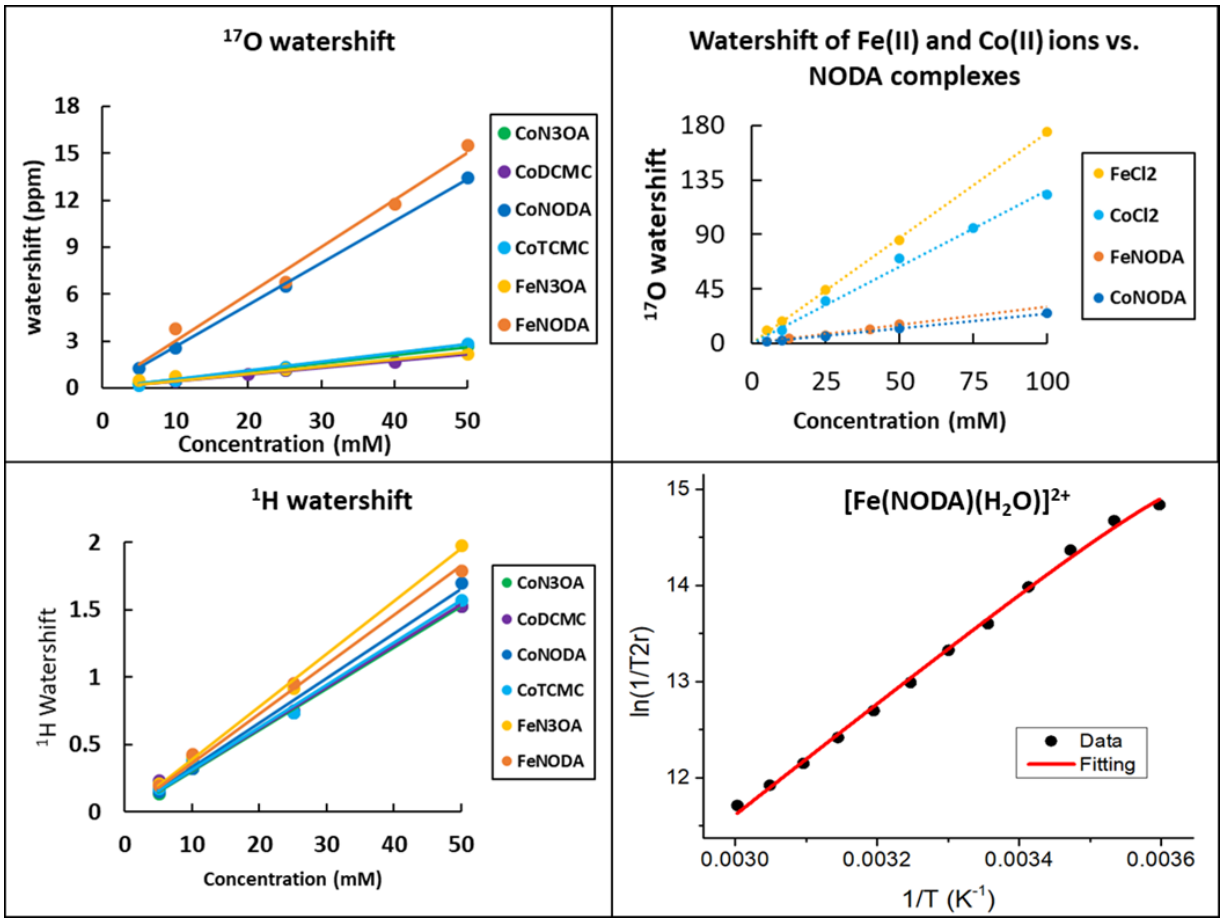

Figure 4. A plot of concentration dependence of ^{17}O water shift of Co(II) and Fe(II) complexes (top left). A ^{17}O water shift plot of Co(II) and Fe(II) NODA complexes and chloride salts at 60˚C (top right). A plot of concentration dependence of ^{1}H water shift of Co(II) and Fe(II) complexes (bottom left). The transverse relaxation of $[Fe(NODA)]^{2+}$ plotted against inverse temperature, fit to the Swift-Connick equations.

A second means of identification of bound water is to plot the ^{17}O NMR water shift as a function of complex concentration at a constant temperature. Figure 4 (top left) shows a plot of the ^{17}O chemical shift of each complex as a function of concentration at 25 °C. The Co(II) and Fe(II) complexes of NODA produce a large shift of the ^{17}O water resonance as a result of direct water coordination, the TCMC, N3OA, and DCMC complexes are poor ^{17}O NMR shift agents as they do not have inner-sphere water. The ^{17}O NMR experimental results correspond to the solid-state structures, which indicate bound water for the NODA complexes.

To approximate the number of bound waters (q), a plot of ^{17}O water shift as a function of $FeCl_2$ and $CoCl_2$ concentration is given for comparison in Figure 4 (top right) and Figures S19-S20.[8] If it is assumed that Co(II) and Fe(II) under these conditions are present as the hexa-aqua complex $[M(OH_2)_6]^{2+}$, then the number of bound water ligands for $[M(NODA)]^{2+}$ is calculated as 1.16 and 1.03 for the cobalt and iron complexes respectively, from the ratio of the slopes. The calculated q values of ~1 further support the hypothesis that the Co(II) and Fe(II) NODA complexes each have a single coordinated water molecule in solution. These experiments to calculate q were carried out at 60 °C for the hexa-aqua complexes to ensure that water exchange was rapid on the NMR time scale.

As shown in Figure 4 (bottom left), the ^{1}H water shift, unlike the ^{17}O water shift did not correlate to the presence of inner-sphere water ligands. All of the cobalt complexes have similar water proton shifts of between 30.5 to 33.1 ppm/M metal complex with the iron complexes $[Fe(N3OA)]^{2+}$ and $([Fe(NODA)]^{2+}$ having slightly larger values of 38.9 and 36.6 ppm/M complex, respectively. This indicates that second sphere and outer-sphere water interactions alone may produce highly paramagnetically shifted water proton resonances, and an inner-sphere water ligand is not requisite.

A Swift-Connick plot[40] of the reduced chemical shift as a function of temperature gives a nearly straight line for $[Fe(NODA)]^{2+}$(Figure 4, bottom right). The positive slope of the plotted data is consistent with a rapidly exchanging water molecule with $k_{ex} > 10^7\ s^{-1}$.[32] An accurate value for the rate constant for exchange cannot be determined in lieu of observation of a more pronounced plateau. For $[Co(NODA)]^{2+}$ a similar plot was observed for a rapidly exchanging water ligand (Figure S21).

Table 2. Magnetic moment (μ_{eff}) was calculated with samples containing 5-50 mM complex, 20 mM pH 7.0 HEPES buffer in 5% by volume t-butanol at 25˚C. The percent CEST, frequency, and exchange rate constants are reported with 10 mM complex, 20 mM HEPES buffer, 100 mM NaCl samples at 37˚C, 28 μT.

Complex	μ_{eff}	CEST (%)	Frequency (ppm)	$k_{ex}(s^{-1})$	Cu^{II} dissociation assay (%)
$[Co(N3OA)]^{2+}$	4.05±0.08	31.9	60	900	~0
$[Co(DCMC)]^{2+}$	4.37±0.32	26.4 ±0.2	65	1230±220	~0
$[Co(NODA)]^{2+}$	4.14±0.12	24.4±0.2	67	1080±30	71.9±2.7
***$[Co(TCMC)]^{2+}$**	4.40±0.21	21.0±0.1	45	300	~0
$[Fe(N3OA)]^{2+}$	4.69±0.10	31.6 ±1.1	67,69	1110	~0
$[Fe(NODA)]^{2+}$	4.54±0.14	22.0±1.0	60	780±10	78.6±5.8

*From reference[16]

The Z-spectra are plotted as the percent reduction of the water proton peak as a function of the presaturation frequency for 1 ppm increments for three Co(II) complexes and for $[Fe(NODA)]^{2+}$ and $[Fe(N3OA)]^{2+}$ (Figure 5). A CEST peak at 60-69 ppm is observed for all complexes except $[Co(TCMC)]^{2+}$. $[Co(TCMC)]^{2+}$ has a less highly shifted CEST peak at 45 ppm. A second amide CEST peak is normally observed for complexes with unsubstituted amide groups with an approximately 60 ppm difference, corresponding to the two magnetically inequivalent NH protons.[18, 41] This peak is observed as a shoulder on the bulk water peak for $[Co(N3OA)]^{2+}$ and $[Co(NODA)]^{2+}$, but is not observed for the other complexes. Presumably, the second CEST peak from the amide protons is buried underneath the water peak. The pH dependence of the CEST peak intensity of all complexes is characteristic of NH amide protons of pendents bound to Co(II). [16-18, 41] The intensity of the furthest shifted CEST peak for these complexes increases from pH 6.7 to 7.6, then decreases in intensity at more basic pH values (Fig. S24, S25). The increase in intensity corresponds to an increase in rate constant for proton exchange in the same pH range, with values as low as 310 s^{-1} at pH 6.9 to 2100 s^{-1} at pH 7.8 (Figure S26-S30 for Omega Plots). The similarity of the z-spectrum of $[Co(NODA)]^{2+}$ to $[Co(N3OA)]^{2+}$ and $[Co(DCMC)]^{2+}$ suggests that the CEST peak is due to the amide protons and not to the water ligand. This assignment is supported by measurements of the rate of water ligand exchange as discussed below.

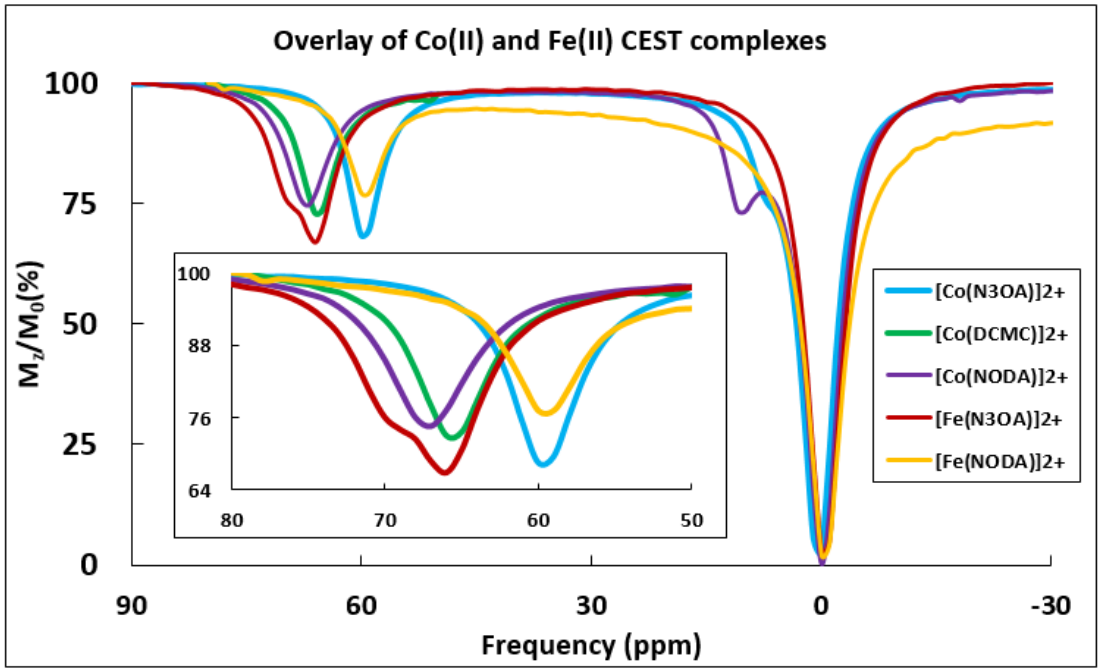

Figure 5. An overlay of $[Co(N3OA)]^{2+}$, $[Co(DCMC)]^{2+}$, $[Co(NODA)]^{2+}$, $[Fe(N3OA)]^{2+}$, and $[Fe(NODA)]^{2+}$ CEST spectra at 37 ^{o}C. Samples contain 10 mM complex, 20 mM HEPES buffer and 100 mM NaCl, and are at pH values of 7.4.

Transmetallation studies of the complexes were carried out with competing Cu(II) ions. Solutions of complexes with 1:1, 2:1, or 4:1 ratios of complex to Cu^{2+} were monitored for three or more hours by observing the formation of Cu(II) complex (Table 2). For the $[Co(N3OA)]^{2+}$, $[Fe(NO3A)]^{2+}$ and $[Co(DCMC)]^{2+}$ complexes, no displacement was observed under these conditions (Figure S31-S34). However, for $[Fe(NODA)]^{2+}$ and $[Co(NODA)]^{2+}$ complexes, significant trans-metallation was observed. Greater than 70% of the Co(II) was displaced from the NODA complex after seven hours with a four-fold excess of Cu(II) whereas 90% of the Fe(II) was displaced form NODA with a four-fold excess of Cu(II) after one hour (Figures S33, S35).

The resistance of Co(II) complexes towards dissociation was compared by incubation under acidic conditions and in the presence of biological anions (Table S17, Figures S36-41). NMR samples containing 3 mM of the internal standard of Sodium 3-trimethylsilyl-1-propanesulfonate (TMPS) were used for the acid and anion dissociation studies. The complexes are very resilient to exposure to acidic conditions (pD 3.5) relative to other published complexes under similar conditions,[18] with no observable change to complexes in a twelve-hour span. In the presence of anions (25 mM carbonate and 1 mM phosphate), some dissociation was observed, however the averages remained below 10% for all

complexes after twelve hours, indicating again that the complexes are relatively inert to loss of metal ion. Most likely, the resistance to dissociation of the complexes in acid or in the presence of anions is a kinetic effect. However, it is possible that thermodynamic stability of the complexes contributes to the observed robustness, as the stability constants under these conditions are not known.

Discussion

The Co(II) and Fe(II) complexes studied here produced Z-spectra that were typical of amide N–H protons of paramagnetic Co(II) or Fe(II) complexes.[15-18, 27, 30, 41] The position of the CEST peak relative to bulk water ranged from 60 to 70 ppm for all complexes, and all had similar intensities and pH dependence. It is remarkable that the CEST peak position varied so little between the complexes despite their different coordination geometries. Notably, these complexes produce improved Z-spectra compared to that of the $[Co(TCMC)]^{2+}$ or $[Fe(TCMC)]^{2+}$ complexes[17] from the standpoint of producing a larger shift of the peak from bulk water and also the larger magnitude of the CEST effect. The N3OA complexes have significantly stronger CEST intensity, resulting from two similar amide peaks that overlap and thus create a greater CEST effect overall. This overlap can be observed best with $[Fe(N3OA)]^{2+}$, where the CEST peak has a shoulder that likely results from two amide peaks that are similar combining to increase the overall intensity of CEST. However, in terms of CEST peak position, the Co(II) complexes that contain macrocycles with 12-membered rings and either six, seven or eight coordination are not the most highly shifted. Co(II) complexes of 14-membered a tetrazamacrocycle with amide pendents, produce highly shifted CEST effect of 120 ppm.[16, 18] Non-macrocyclic ligands with pendent amide also show highly shifted CEST peaks at 100 ppm.[42] However, the kinetic inertness and thermodynamic stability of the 12-membered macrocyclic complexes make them desirable candidates for applications that require robust complexes.

One such application is the development of paramagnetic water shift reagents for nano-carrier CEST agents.[10, 12, 14] Initially, we assumed that an inner-sphere water was necessary for a water proton shift agent and focused on forming complexes with water ligands. The ^{17}O NMR studies were consistent with the Co(II) and Fe(II) NODA complexes containing an inner-sphere water ligand, the only complexes here that had a bound water. Previous pH –potentiometric studies in our laboratory showed that there were no ligand ionizations occurring until above a pH of 8 for the Co(II) NODA complex.[43] This result suggests that, at neutral pH, $[Co(NODA)(OH_2)]^{2+}$ is the predominant species. In other words, water and not hydroxide is bound to Co(II) at near neutral pH. Fitting a variable temperature transverse relaxation

plot from variable temperature ^{17}O NMR experiments to the Swift-Connick equations allowed us to estimate that the k_{ex} of water ligand was greater than 10^7 s^{-1} for the Fe(II)complex. A similar plot was observed for the Co(II) complex. In comparison, TACN-based six-coordinate Co(II) complexes have smaller rate constants for water exchange on the order of 10^6 s^{-1}.[8] A seven coordinate complex of Fe(II) with polyaminocarboxylate ligand has a rate constant for water ligand exchange of 3 x 10^7 s^{-1}. [33]

Other complexes studied here had a more limited effect on the ^{17}O water resonance, indicating that there was no directly bound water to metal center, and that contributions were mainly outer-sphere. There was very little difference in proton water shift produced by the different complexes, indicating that second sphere interactions are the major contributor of water shift. This highlights the fact that direct interaction of a paramagnetic metal and water is not necessary for producing large paramagnetically shifted water ^1H resonances. Second sphere water interactions in transition metal complexes are enhanced with donor groups such as amides or alcohols that form hydrogen bonds to water.[8] Notably, chemists who design metal complex probes have sought to balance stability and water interaction of these complexes for applications as MRI agents.[44-45] At least in this example, direct inner-sphere water interaction did not significantly improve proton resonance shift. For prioritization of inertness and stability, a closed coordination sphere is advantageous.

It is interesting to compare the coordination number and geometries of these complexes with analogous ones reported in the literature. For example, the Co(II) complex of TCMC shows both six-coordinate and 7-coordinate structures that correspond quite closely to those of $[Co(DCMC)]^{2+}$ and $[Co(N3OA)]^{2+}$ respectively, with nearly identical coordination geometry.[18] Notably, the Mn(II) complex with the ligand 1,7-DO2A (the DCMC analog with acetate pendents) is also six coordinate with an absence of water ligands.[22, 46] The Mn(II) and Fe(II) complexes of TCMC are both eight coordinate as shown by crystallography.[18, 22] Yet, the Fe(II) complex of N3OA appears to be seven coordinate in solution with a lack of water ligands as supported by proton NMR data and ^{17}O NMR analysis.

The NODA complexes are distinct from the other two macrocyclic complexes in that a solvent molecule occupies a seventh coordination site. Both the Fe(II) and Co(II) complexes have a seven coordinate structure and are close to a distorted pentagonal bipyramidal geometry, with pseudo-axial bond angles of 176.4 and 168.23 respectively, close to the ideal of 180°. The iron complex structure is particularly interesting as 7-coordinate Fe(III) structures are quite rare, although a few have been reported.[47-48]

As shown here, some ligands based on 12-membered macrocycles produce extremely stable Fe(II) complexes and others produce Fe(II) complexes that are readily oxidized. The Fe(II) complex of

TCMC is eight coordinate and is correspondingly very inert towards dissociation as the metal ion is totally encapsulated by the macrocycle.[23] $[Fe(TCMC)]^{2+}$ is also very resistant to oxidation. This may be attributed in part to the longer Fe-N and Fe-O bond lengths that would favor the larger Fe(II) ion over the Fe(III) ion. Removal of one pendent group to produce $[Fe(NO3A)]^{2+}$ produces a complex that remains inert towards trans-metalation and also towards oxidation. However, removal of two pendent amide groups to give $[Fe(DCMC)]^{2+}$ produces a complex that is very prone to oxidation. Notably, the seven coordinate $[Fe(NODA)(OH^2)]^{2+}$ is relatively resistant to oxidation to Fe(III), at least at neutral pH. Higher pH values would be expected to produce the hydroxide complex which would favor oxidation to Fe(III).

Summary. Co(II) and Fe(II) complexes of 12-membered macrocyclic ligands show promise for CEST applications including shift reagents for bulk water and as paraCEST agents. We attempted to produce several examples of complexes with inner-sphere water ligands, but only found two examples including one each of Co(II) and Fe(II). Notably, it is not straightforward to predict coordination number for Co(II) and Fe(II) complexes of ligands based on the 12-membered-aza macrocycles with variable pendent groups. Similar observations have been made with Mn(II) complexes that are under development as T_1 MRI contrast agents.[22, 49-52] These Mn(II) complexes range in coordination number from six to eight. However, as shown here, Co(II) and Fe(II) complexes with amide pendents produce large proton water shifts even in the absence of inner-sphere water molecules. This feature will be useful in the development of paramagnetic transition metal complexes for cellCEST or lipoCEST.[14] Complexes that lack an innersphere water are remarkably stable towards dissociation and oxidation at neutral pH and are good candidates for further development.

Associated content

Supporting information

The supporting information is free of charge on the ACS publications website at DOI xx.
Experimental details including NMR spectra, CEST spectra, Omega plots to obtain exchange rate constants and synthetic procedures are available.

Author information

Corresponding author

Email: jmorrow@buffalo.edu , fax 716-645-6963

Acknowledgements

JRM thanks the NSF (CHE-1310374 and CHE-1710224) for support of this work. R.M. thanks the Fulbright Commission in India via USIEF for a fellowship. MRC thanks SUNY Fredonia for the use of their diffractometer. We thank Professors Timothy R. Cook and David F. Watson for use of their electrochemistry equipment.

References

1. Wahsner, J.; Gale, E. M.; Rodriguez-Rodriguez, A.; Caravan, P., Chemistry of MRI Contrast Agents: Current Challenges and New Frontiers. *Chem Rev* **2018,** *119* (2), 957-1057.
2. Terreno, E.; Castelli, D. D.; Viale, A.; Aime, S., Challenges for molecular magnetic resonance imaging. *Chem Rev* **2010,** *110* (5), 3019-42.
3. Botta, M., Second coordination sphere water molecules and relaxivity of gadolinium(III) complexes: implications for MRI contrast agents. *Eur. J. Inorg. Chem.* **2000**, 399-407.
4. Aime, S.; Baroni, S.; Delli Castelli, D.; Brucher, E.; Fabian, I.; Serra, S. C.; Fringuello Mingo, A.; Napolitano, R.; Lattuada, L.; Tedoldi, F.; Baranyai, Z., Exploiting the Proton Exchange as an Additional Route to Enhance the Relaxivity of Paramagnetic MRI Contrast Agents. *Inorg Chem* **2018,** *57* (9), 5567-5574.
5. Carnovale, I. M.; Lolli, M. L.; Serra, S. C.; Mingo, A. F.; Napolitano, R.; Boi, V.; Guidolin, N.; Lattuada, L.; Tedoldi, F.; Baranyai, Z.; Aime, S., Exploring the intramolecular catalysis of the proton exchange process to modulate the relaxivity of Gd(iii)-complexes of HP-DO3A-like ligands. *Chem Commun (Camb)* **2018,** *54* (72), 10056-10059.
6. Cakic, N.; Tickner, B.; Zaiss, M.; Esteban-Gomez, D.; Platas-Iglesias, C.; Angelovski, G., Spectrally Undiscerned Isomers Might Lead to Erroneous Determination of Water Exchange Rates of paraCEST Eu(III) Agents. *Inorganic Chemistry* **2017,** *56* (14), 7737-7745.
7. Abozeid, S. M.; Snyder, E. M.; Lopez, A. P.; Steuerwald, C. M.; Sylvester, E.; Ibrahim, K. M.; Zaky, R. R.; Abou-El-Nadar, H. M.; Morrow, J. R., Nickel(II) Complexes as Paramagnetic Shift and paraCEST Agents. *Eur J Inorg Chem* **2018,** (18), 1902-1908.
8. Abozeid, S. M.; Snyder, E. M.; Tittiris, T. Y.; Steuerwald, C. M.; Nazarenko, A. Y.; Morrow, J. R., Inner-Sphere and Outer-Sphere Water Interactions in Co(II) paraCEST Agents. *Inorg Chem* **2018,** *57* (4), 2085-2095.
9. Huang, C. H.; Hammell, J.; Ratnakar, S. J.; Sherry, A. D.; Morrow, J. R., Activation of a PARACEST agent for MRI through selective outersphere interactions with phosphate diesters. *Inorg Chem* **2010,** *49* (13), 5963-70.
10. Castelli, D. D.; Terreno, E.; Longo, D.; Aime, S., Nanoparticle-based chemical exchange saturation transfer (CEST) agents. *Nmr Biomed* **2013,** *26* (7), 839-849.
11. Opina, A. C. L.; Ghaghada, K. B.; Zhao, P. Y.; Kiefer, G.; Annapragada, A.; Sherry, A. D., TmDOTA-Tetraglycinate Encapsulated Liposomes as pH-Sensitive LipoCEST Agents. *Plos One* **2011,** *6* (11).
12. Ferrauto, G.; Carniato, F.; Tei, L.; Hu, H.; Aime, S.; Botta, M., MRI nanoprobes based on chemical exchange saturation transfer: Ln(III) chelates anchored on the surface of mesoporous silica nanoparticles. *Nanoscale* **2014,** *6* (16), 9604-9607.
13. Ferrauto, G.; Di Gregorio, E.; Baroni, S.; Aime, S., Frequency-Encoded MRI-CEST Agents Based on Paramagnetic Liposomes/RBC Aggregates. *Nano Lett* **2014,** *14* (12), 6857-6862.
14. Ferrauto, G.; Castelli, D. D.; Di Gregorio, E.; Terreno, E.; Aime, S., LipoCEST and cellCEST imaging agents: opportunities and challenges. *Wiley Interdisciplinary Reviews-Nanomedicine and Nanobiotechnology* **2016,** *8* (4), 602-618.
15. Dorazio, S. J.; Morrow, J. R., Iron(II) Complexes Containing Octadentate Tetraazamacrocycles as ParaCEST Magnetic Resonance Imaging Contrast Agents. *Inorganic Chemistry* **2012,** *51* (14), 7448-7450.
16. Dorazio, S. J.; Olatunde, A. O.; Spernyak, J. A.; Morrow, J. R., CoCEST: cobalt(II) amide-appended paraCEST MRI contrast agents. *Chem Commun* **2013,** *49* (85), 10025-10027.
17. Dorazio, S. J.; Olatunde, A. O.; Tsitovich, P. B.; Morrow, J. R., Comparison of divalent transition metal ion paraCEST MRI contrast agents. *J. Biol. Inorg. Chem.* **2014,** *19* (2), 191-205.

18. Olatunde, A. O.; Bond, C. J.; Dorazio, S. J.; Cox, J. M.; Benedict, J. B.; Daddario, M. D.; Spernyak, J. A.; Morrow, J. R., Six, Seven or Eight Coordinate Fe-II, Co-II or Ni-II Complexes of Amide-Appended Tetraazamacrocycles for ParaCEST Thermometry. *Chem-Eur J* **2015,** *21* (50), 18290-18300.
19. Tsitovich, P. B.; Cox, J. M.; Spernyak, J. A.; Morrow, J. R., Gear Up for a pH Shift: A Responsive Iron(II) 2-Amino-6-picolyl-Appended Macrocyclic paraCEST Agent That Protonates at a Pendent Group. *Inorg Chem* **2016,** *55* (22), 12001-12010.
20. Tsitovich, P. B.; Gendron, F.; Nazarenko, A. Y.; Livesay, B. N.; Lopez, A. P.; Shores, M. P.; Autschbach, J.; Morrow, J. R., Low-Spin Fe(III) Macrocyclic Complexes of Imidazole-Appended 1,4,7-Triazacyclononane as Paramagnetic Probes. *Inorg Chem* **2018,** *57* (14), 8364-8374.
21. Burns, P. J.; Cox, J. M.; Morrow, J. R., Imidazole-Appended Macrocyclic Complexes of Fe(II), Co(II), and Ni(II) as ParaCEST Agents. *Inorg Chem* **2017,** *56* (8), 4546-4555.
22. Wang, S.; Westmoreland, T. D., Correlation of Relaxivity with Coordination Number in Six-, Seven-, and Eight-Coordinate Mn(II) Complexes of Pendant-Arm Cyclen Derivatives. *Inorganic Chemistry* **2009,** *48* (2), 719-727.
23. Dorazio, S. J.; Tsitovich, P. B.; Gardina, S. A.; Morrow, J. R., The reactivity of macrocyclic Fe(II) paraCEST MRI contrast agents towards biologically relevant anions, cations, oxygen or peroxide. *J Inorg Biochem* **2012,** *117*, 212-9.
24. Tsitovich, P. B.; Morrow, J. R., Macrocyclic ligands for Fe(II) paraCEST and chemical shift MRI contrast agents. *Inorganica Chimica Acta* **2012,** *393*, 3-11.
25. Tsitovich, P. B.; Tittiris, T. Y.; Cox, J. M.; Benedict, J. B.; Morrow, J. R., Fe(ii) and Co(ii) N-methylated CYCLEN complexes as paraSHIFT agents with large temperature dependent shifts. *Dalton Trans* **2018,** *47* (3), 916-924.
26. Tsitovich, P. B.; Cox, J. M.; Benedict, J. B.; Morrow, J. R., Six-coordinate Iron(II) and Cobalt(II) paraSHIFT Agents for Measuring Temperature by Magnetic Resonance Spectroscopy. *Inorg Chem* **2016,** *55* (2), 700-16.
27. Srivastava, K.; Ferrauto, G.; Young, V. G., Jr.; Aime, S.; Pierre, V. C., Eight-Coordinate, Stable Fe(II) Complex as a Dual (19)F and CEST Contrast Agent for Ratiometric pH Imaging. *Inorg Chem* **2017,** *56* (20), 12206-12213.
28. Srivastava, K.; Weitz, E. A.; Peterson, K. L.; Marjanska, M.; Pierre, V. C., Fe- and Ln-DOTAm-F12 Are Effective Paramagnetic Fluorine Contrast Agents for MRI in Water and Blood. *Inorg Chem* **2017,** *56* (3), 1546-1557.
29. Dorazio, S. J.; Morrow, J. R., Iron(II) complexes containing octadentate tetraazamacrocycles as paraCEST magnetic resonance imaging contrast agents. *Inorg Chem* **2012,** *51* (14), 7448-50.
30. Dorazio, S. J.; Tsitovich, P. B.; Siters, K. E.; Spernyak, J. A.; Morrow, J. R., Iron(II) PARACEST MRI contrast agents. *J Am Chem Soc* **2011,** *133* (36), 14154-6.
31. Tsitovich, P. B.; Tittiris, T. Y.; Cox, J. M.; Benedict, J. B.; Morrow, J. R., Fe(II) and Co(II) N-methylated CYCLEN complexes as paraSHIFT agents with large temperature dependent shifts. *Dalton T* **2018,** *47* (3), 916-924.
32. Maigut, J.; Meier, R.; Zahl, A.; van Eldik, R., Elucidation of the solution structure and water-exchange mechanism of paramagnetic [Fe-II(edta)(H2O)](2-). *Inorganic Chemistry* **2007,** *46* (13), 5361-5371.
33. Maigut, J.; Meier, R.; Zahl, A.; van Eldik, R., Effect of chelate dynamics on water exchange reactions of paramagnetic aminopolycarboxylate complexes. *Inorg Chem* **2008,** *47* (13), 5702-19.
34. Jeon, I.-R.; Park, J. G.; Haney, C. R.; Harris, T. D., Spin Crossover iron(II) complexes as PARACEST MRI thermometers. *Chem. Sci.* **2014,** *5*, 2461-2465.
35. Torardi, C. C.; Brixner, L. H.; Blasse, G., Structure and luminescence of K2TaF7 and K2NbF7. *J. Solid State Chem.* **1987,** *67* (1), 21-25.

36. Barefield, E. K.; Busch, D. H., Iron, cobalt and nickel complexes having anomalous magnetic moments. *Q. Rev. Chem. Soc.* **1968,** *22*, 457-498.
37. Kuznik, N.; Wyskocka, M., Iron(III) contrast agent candidates for MRI: a survey of the structure-effect relaitonship in the last 15 years of studies. *Eur. J. Inorg. Chem.* **2016**, 445-458.
38. Caneschi, A.; Dei, A.; Gatteschi, D.; Tangoulis, V., Antiferromagnetic coupling in a six-coordinate high spin cobalt(II)-semiquinonato complex. *Inorg Chem* **2002,** *41* (13), 3508-12.
39. Harris, D. C., *Quantitative Chemical Analysis*. 8th ed.; W. H. Freeman and Company: New York, NY, 2010.
40. Swift, T. J.; Connick, R. E., NMR-relaxation mechanisms of O-17 in aqueous solutions of paramagnetic cations and the lifetime of water molecules in the first coordination sphere. *J. Chem. Phys. 1962* **1962,** *37* (2), 307-320.
41. Olatunde, A. O.; Cox, J. M.; Daddario, M. D.; Spernyak, J. A.; Benedict, J. B.; Morrow, J. R., Seven-coordinate Co(II), Fe(II) and six-coordinate Ni(II) amide-appended macrocyclic complexes as ParaCEST agents in biological media. *Inorg Chem* **2014,** *53* (16), 8311-21.
42. Thorarinsdottir, A. E.; Du, K.; Collins, J. H. P.; Harris, T. D., Ratiometric pH Imaging with a Co(II)2 MRI Probe via CEST Effects of Opposing pH Dependences. *J Am Chem Soc* **2017,** *139* (44), 15836-15847.
43. Tittiris, T. Y., University at Buffalo, Ph.D. Thesis. **2017**.
44. Di Gregorio, E.; Ferrauto, G.; Furlan, C.; Lanzardo, S.; Nuzzi, R.; Gianolio, E.; Aime, S., The Issue of Gadolinium Retained in Tissues: Insights on the Role of Metal Complex Stability by Comparing Metal Uptake in Murine Tissues Upon the Concomitant Administration of Lanthanum- and Gadolinium-Diethylentriamminopentaacetate. *Invest Radiol* **2018,** *53* (3), 167-172.
45. Le Fur, M.; Caravan, P., The biological fate of gadolinium-based MRI contrast agents: a call to action for bioinorganic chemists. *Metallomics* **2019,** *11* (2), 240-254.
46. Rolla, G. A.; Platas-Iglesias, C.; Botta, M.; Tei, L.; Helm, L., H-1 and O-17 NMR Relaxometric and Computational Study on Macrocyclic Mn(II) Complexes. *Inorganic Chemistry* **2013,** *52* (6), 3268-3279.
47. Williams, N. J.; Dean, N. E.; VanDerveer, D. G.; Luckay, R. C.; Hancock, R. D., Strong metal ion size based selectivity of the highly preorganized ligand PDA (1,10-phenanthroline-2,9-dicarboxylic acid) with trivalent metal ions. A crystallographic, fluorometric, and thermodynamic study. *Inorg Chem* **2009,** *48* (16), 7853-63.
48. Craig, G. A.; Barrios, L. A.; Sanchez Costa, J.; Roubeau, O.; Ruiz, E.; Teat, S. J.; Wilson, C. C.; Thomas, L.; Aromi, G., Synthesis of a novel heptacoordinated Fe(III) dinuclear complex: experimental and theoretical study of the magnetic properties. *Dalton Trans* **2010,** *39* (20), 4874-81.
49. Rolla, G. A.; Platas-Iglesias, C.; Botta, M.; Tei, L.; Helm, L., 1H and 17O NMR relaxometric and computational study on macrocyclic Mn(II) complexes. *Inorg Chem* **2013,** *52* (6), 3268-79.
50. Forgacs, A.; Tei, L.; Baranyai, Z.; Esteban-Gomez, D.; Platas-Iglesias, C.; Botta, M., Optimising the relaxivities of Mn(2+) complexes by targeting human serum albumin (HSA). *Dalton Trans* **2017,** *46* (26), 8494-8504.
51. Garda, Z.; Molnar, E.; Kalman, F. K.; Botar, R.; Nagy, V.; Baranyai, Z.; Brucher, E.; Kovacs, Z.; Toth, I.; Tircso, G., Effect of the Nature of Donor Atoms on the Thermodynamic, Kinetic and Relaxation Properties of Mn(II) Complexes Formed With Some Trisubstituted 12-Membered Macrocyclic Ligands. *Front Chem* **2018,** *6*, 232.
52. Forgacs, A.; Tei, L.; Baranyai, Z.; Toth, I.; Zekany, L.; Botta, M., A bisamide derivative of [MN(1,4-DO2A)]-solution themodynamic, kinetic and NMR relaxometri studies. *Eur. J. Inorg. Chem.* **2016**, 1165-1174.

For table of contents only

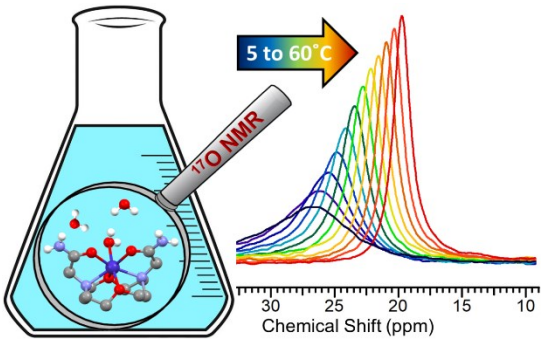

Fe(II) and Co(II) complexes of 12-membered macrocycles containing amide pendents produce paramagnetically shifted bulk water or macrocyclic ligand ^{1}H resonances for CEST MRI applications. Complexes with inner-sphere water ligands show little advantage over those lacking water ligands and, in the case of Fe(II), produce probes that more readily oxidize to Fe(III).